Power Coordinates: A Geometric Construction of Barycentric Coordinates on Convex Polytopes

Max Budninskiy, Caltech
Beibei Liu, Caltech
Yiying Tong, MSU
Mathieu Desbrun, Caltech

Abstract

We present a full geometric parameterization of generalized barycentric coordinates on convex polytopes. We show that these continuous and non-negative coefficients ensuring linear precision can be efficiently and exactly computed through a power diagram of the polytope's vertices and the evaluation point. In particular, we point out that well-known explicit coordinates such as Wachspress, Discrete Harmonic, Voronoi, or Mean Value correspond to simple choices of power weights. We also present examples of new barycentric coordinates, and discuss possible extensions such as power coordinates for non-convex polygons and smooth shapes.

Keywords: Generalized barycentric coordinates, Wachspress and mean-value coordinates, power diagrams, polytopal finite elements.

Concepts: •**Computing methodologies** → **Shape modeling;** •**Theory of computation** → **Computational geometry;**

1 Introduction

Generalized barycentric coordinates extend the canonical case of Möbius' barycentric coordinates on simplices: they offer a simple and powerful way to interpolate values on a polygonal (2D) or polytopal (3D) convex domain through a weighted combination of values associated with the polytope vertices. From values of a given function Φ at vertices $\mathbf{v}_i$, one obtains a straightforward interpolating function ϕ via:

$$\phi(\mathbf{x}) = \sum_{i=1}^{n} \lambda_i(\mathbf{x})\ \Phi(\mathbf{v}_i). \tag{1}$$

where the weights $\{\lambda_i\}_{i=1..n}$ are functions of $\mathbf{x}$ that are often referred to as generalized barycentric coordinates.

While interpolation over simplicial (via linear basis functions) or quadrilateral/hexahedral (via multilinear basis functions) elements has been used for decades in finite element computations and graphics, a strong interest in the design of more general interpolants recently surfaced in various disciplines such as geometric modeling (for Bézier patches, mesh parameterization, and volumetric deformation), image processing (for image deformation) and computational physics (to define basis functions on polytopal elements). Among the many possible choices of coordinates that are known today, Wachspress coordinates [Wachspress 1975; Meyer et al. 2002; Warren et al. 2006] have been widely adopted in 2D and 3D as they possess simple closed forms and produce natural-looking interpolations in arbitrary convex domains due to being rational polynomials of minimal degree [Warren 2003]. Mean value coordinates [Floater 2003; Floater et al. 2005] are also very useful as they behave nicely even on non-convex polytopes [Hormann and Floater 2006], making them particularly convenient for cage-based shape deformation [Ju et al. 2005b].

These two most-common coordinates have recently been extended to spherical domains [Langer et al. 2006], to smooth shapes [Schaefer et al. 2007], and even to the Hermite setting [Dyken and Floater 2009]. Yet, the existence and construction of other generalized coordinates on convex polytopes remain relevant in geometric modelling [Varady et al. 2016] or even in finite element computations [Gillette et al. 2016], where convex elements are still strongly preferred to ensure discrete maximum properties. The goal of this paper is to propose a principled geometric approach to characterize, design and compute coordinates on convex polytopes that provably satisfy the key properties expected from barycentric coordinates.

1.1 Problem statement

This paper focuses mainly on polytopal barycentric coordinates in $\mathbb{R}^d$ ($d = 2, 3$). Let $\mathcal{P}$ be a non-degenerate convex polytope with n vertices $\mathbf{V} = \{\mathbf{v}_1, ..., \mathbf{v}_n\}$. We further assume that these vertices are all extreme points of the polytope, that is, no vertex is a convex combination of the other vertices. Note that this implies that the discrete Gaussian curvature of each vertex is strictly positive. Functions $\{\lambda_i : \mathbb{R}^d \to \mathbb{R}\}_{i=1..n}$ are called barycentric coordinates if they satisfy the following properties:

- **Partition of unity**:
$$\sum_{i=1..n} \lambda_i(\mathbf{x}) = 1 \quad \forall\, \mathbf{x} \in \mathcal{P} \tag{a}$$
- **Linear precision**:
$$\sum_{i=1..n} \lambda_i(\mathbf{x})\ \mathbf{v_i} = \mathbf{x} \quad \forall\, \mathbf{x} \in \mathcal{P} \tag{b}$$
- **Non-negativity** inside the convex polytope $\mathcal{P}$:
$$\forall\, i \in [1..n], \quad \lambda_i(\mathbf{x}) \geq 0 \quad \forall \mathbf{x} \in \mathcal{P} \tag{c}$$
- **Smoothness** away from vertices:
$$\forall\, i \in [1..n], \quad \lambda_i(\cdot) \in C^k\big(\mathcal{P} \backslash \cup_j \{\mathbf{v}_j\}\big). \tag{d}$$

In previous work, additional properties are often required of barycentric coordinates as well, including:

- Exact interpolation of nodal data (Lagrange property):
$$\forall i, j \in [1..n], \quad \lambda_i(\mathbf{v}_j) = \delta_{ij} \tag{e}$$
- Restriction on facets of $\partial\mathcal{P}$:
$$\text{For a facet } \mathcal{F} = \mathrm{Conv}\big(\mathbf{v}_{i_1}, \ldots, \mathbf{v}_{i_m}\big) \subset \partial\mathcal{P},$$
$$\forall j \notin \{i_1, \ldots, i_m\}, \quad \lambda_j(\mathbf{x}) = 0 \quad \forall \mathbf{x} \in \mathcal{F}. \tag{f}$$

However, the Lagrange property (e) and the property (f) of reduction to linearly-precise coordinates on the boundary faces of $\mathcal{P}$ are

SIGGRAPH Asia 2016, December 5-8, 2016, Macau
ISBN: 978-1-4503-4514-9/16/12
DOI: http://dx.doi.org/10.1145/2980179.2982441

mere consequences of the requirements (a)–(d) for convex polytopes (see App. A). Generalized barycentric coordinates satisfying all these requirements are particularly desirable in a wide variety of applications: they enforce exact interpolation at vertices, offer a discrete maximum principle for interpolants, guarantee convergence of the Galerkin method for second-order PDEs, and so on [Floater 2015]. Despite their apparent simplicity, enforcing *all* these conditions is remarkably difficult as we now briefly review.

1.2 Previous work

While a thorough survey on generalized coordinates can be found in [Floater 2015], we briefly review previous approaches that have been proposed over the years to better position our contributions.

Early developments for convex polytopes. Motivated by the design of basis functions over convex polygons, Wachspress [1975] proposed a general construction of rational polynomial basis functions using projective geometry. This generalization of barycentric coordinates was further analyzed and extended to higher dimensions by Warren [Warren 2003], and its use in graphics (along with simple 2D and 3D evaluations) was advocated in [Meyer et al. 2002; Warren et al. 2006]. Weighted averages of simplicial barycentric coordinates were also introduced by Floater [1997] for parameterization purposes, but these coordinates were only C^0. The cotangent weights used for the Laplacian operator [Meyer et al. 2002] (often referred to as "discrete harmonic weights" [Eck et al. 1995]) were also noted as valuable, but fail to satisfy positivity (c). In the context of finite elements, the work of Malsch and Dasgupta [2004; 2005] extended Wachspress approach to weakly convex polygons and convex polygons with interior nodes.

Extensions to arbitrary polytopes. Recognizing that classical forms of coordinates often lose smoothness or are not well-defined when applied to a non-convex polytope, Floater introduced Mean Value Coordinates (MVC [Floater 2003]). These coordinates still have a simple expression that is easily evaluated, and while they fail to offer positivity on concave polytopes, they remain well defined everywhere in the plane given arbitrary polygonal domains [Hormann and Floater 2006]. Floater et al. [2006] showed that while the three most common existing generalized coordinates are part of a larger family, only two of them, namely MVC and Wachspress, satisfy requirements (c)–(f) for convex polytopes. A number of approaches have also explored the design of coordinates on non-convex polytopes by relaxing some of the barycentric requirements. When coordinates are used for deformation for instance, removing the Lagrange property and extending the coordinates to be complex valued (or, equivalently, matrix valued) allow for a minimization of angle distortion [Weber et al. 2009; Weber and Gotsman 2010; Lipman et al. 2008]. Mean value coordinates can also be seen as a case where positivity is no longer required for non-convex polytopes, a goal targeted in [Manson and Schaefer 2010] as well. Instead, Positive Gordon-Wixom coordinates [Manson et al. 2011] do achieve positivity for arbitrary polygons, but are only C^0.

Non-analytical coordinates. Several coordinates have been introduced lately to achieve stronger properties. Harmonic coordinates [Joshi et al. 2007], for instance, proposed the use of harmonic weights (satisfying $\Delta\lambda_i = 0$ inside the domain) to enforce positivity for arbitrary polytopes. Positive Mean Value coordinates [Lipman et al. 2007] also stay, by construction, positive on non-convex polytopes. Barycentric coordinates deriving from numerical optimization have also been proposed, such as the interpolatory maximum entropy coordinates [Hormann and Sukumar 2008]. However, these specific methods involve *inexact evaluation* as they require quadratures, optimization, or large memory footprint to store PDE solutions. Their analysis is often more difficult as well.

Further extensions. The idea of generalized coordinates for polytopes has been extended to smooth closed domains, see [Warren et al. 2006; Belyaev 2006; Schaefer et al. 2007]. Multiple methods also extended mean-value coordinates to the Hermite setting [Manson and Schaefer 2010; Weber et al. 2012; Li et al. 2013] when both values and gradients (i.e., normal derivatives) on the boundary need to be interpolated. It was also recognized in [Zhang et al. 2014] that localized influence of a given vertex of the polytope on the interpolation may be beneficial in some applications, bringing forward the idea of *local* coordinates.

Related works. Finally, there are a few applications that share commonalities with our work due to the generality of the concept of barycentric coordinates. For instance, methods for scattered data interpolation such as Shepard [Shepard 1968] and natural neighbors [Sibson 1981] bear significant similarities with barycentric coordinates: e.g., the *Laplace interpolant* variant of natural neighbors is linked to the discrete harmonic barycentric coordinates [Hiyoshi and Sugihara 1999; Cueto et al. 2003]. The finite element literature is also brimming with discussions of various properties of barycentric coordinates on polytopes [Milbradt and Pick 2008].

1.3 Contributions

Despite significant advances in extending barycentric coordinates, only a few coordinates verifying conditions (a)–(f) on convex polytopes are known. In this paper, we exploit an equivalence between generalized coordinates and orthogonal dual diagrams to formulate a full geometric parameterization of barycentric coordinates via power diagrams. We also show how our formulation induces a simple, exact and efficient evaluation of coordinates that leverages robust computational geometry tools. Furthermore, we present how to design customized coordinates through simple weight functions per vertex of the polytope. Finally, we discuss how to extend our approach to non-convex polytopes and arbitrary shapes.

2 Power Coordinates for Convex Polytopes

We begin our exposition by establishing a relationship between generalized barycentric coordinates and power diagrams, providing a geometric (as opposed to analytical [Floater et al. 2006]) characterization of arbitrary coordinates on convex polytopes.

2.1 Background

Given a set of sites $\{\mathbf{x}_k\}_{k=1..n}$ in $\mathbb{R}^d$ and associated scalar weights $\{w_k\}_{k=1..n}$, the *power diagram* of these weighted points is a tessellation in which each convex cell $\mathcal{D}_i$ is defined as:

$$\mathcal{D}_i = \{\mathbf{x} \in \mathbb{R}^d \mid |\mathbf{x}-\mathbf{x}_i|^2 - w_i \leq |\mathbf{x}-\mathbf{x}_k|^2 - w_k \ \forall k\},$$

where $|\cdot|$ indicates the Euclidean norm. Note that when weights are all equal, power diagrams reduce to Voronoi diagrams.

Properties. Cells are guaranteed to be convex and have straight edges. Note that some cells may be empty as well. Two sites $\mathbf{x}_i$ and $\mathbf{x}_j$ are said to be neighbors if the intersection $\mathcal{D}_i \bigcap \mathcal{D}_j$ is a non-empty power facet f_{ij} of codimension 1, corresponding to a planar polygon in 3D (see inset) and a line segment in 2D. We use l_{ij}

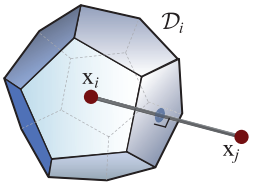

to indicate the distance $|\mathbf{x}_i - \mathbf{x}_j|$, and denote d_{ij} the signed distance from $\mathbf{x}_i$ to f_{ij} so that $d_{ij} + d_{ji} = l_{ij}$. The expression of the distance from a site to a power facet is actually known analytically:

$$d_{ij} = \frac{|\mathbf{x}_i - \mathbf{x}_j|^2 + (w_i - w_j)}{2|\mathbf{x}_i - \mathbf{x}_j|}. \quad (2)$$

Finally, $|f_{ij}|$ denotes the volume of f_{ij} (area in 3D, and length in 2D). Akin to the famous Voronoi-Delaunay duality, a power diagram also defines by duality a triangulation of the sites, known as the regular (or weighted Delaunay) triangulation, in which each neighboring pair of sites forms an edge that is *orthogonal* to its associated power facet. In fact, all possible orthogonal primal-dual pairs corresponding to points $\{\mathbf{x}_k\}_{k=1..n}$ are completely parameterized by weights $\{w_k\}_{k=1..n}$; see, e.g., [Memari et al. 2012]. Furthermore, the weighted circumcenters of the tetrahedra of this regular triangulation in 3D (resp., triangles in 2D, see Fig. 1(left)) correspond to dual vertices of the power diagram, i.e., they are at the intersection of four power cells in 3D (resp., three in 2D). The closed-form expression of the weighted circumcenter $\mathbf{c}^w$ of a p-dimensional simplex σ_p of $\mathcal{T}$ ($p = 1 \dots d$) is:

$$\mathbf{c}^w(\sigma_p) = \mathbf{x}_i + \frac{1}{2\ p\ |\sigma_p|} \sum_{\mathbf{x}_j \in \sigma_p} \left(|\mathbf{x}_i - \mathbf{x}_j|^2 + w_i - w_j\right) \mathbf{N}^{\hat{j}}_{\sigma_p}, \quad (3)$$

where $\mathbf{N}^{\hat{j}}_{\sigma_p}$ is the inward-pointing normal of the face of σ_p opposite to $\mathbf{x}_j$, weighted by the volume of that face.

Gauge and translation. As Eqs. (2) and (3) indicate, adding a constant shift to all the weights does not influence the diagram, so the weights are defined up to a constant. Moreover, adding a linear function $\mathbf{t} \cdot \mathbf{x}_i$ to each weight w_i will only induce a global translation $-\mathbf{t}$ of the power diagram [Memari et al. 2012]. Thus, the geometry of the power diagram has a $(d+1)$–parameter gauge.

2.2 From coordinates to power diagrams

Power diagrams have found a variety of applications in geometry processing [Mullen et al. 2011; de Goes et al. 2012; de Goes et al. 2013; Liu et al. 2013; Budninskiy et al. 2016] and animation [Busaryev et al. 2012; de Goes et al. 2015]. As we now review, they are also intimately linked to barycentric coordinates. Even if our exposition focuses on 2D and 3D, the results of this section are general and hold in arbitrary dimension.

Homogeneous coordinates. Given a convex polytope $\mathcal{P}$ with vertices $\{\mathbf{v}_i\}_{i=1..n}$, the *homogeneous coordinates* of $\mathcal{P}$ [Floater 2015] are a set of functions $\{h_i : \mathbb{R}^d \to \mathbb{R}\}_{i=1..n}$ that satisfy the following property:

$$\sum_{i=1..n} h_i(\mathbf{x})(\mathbf{v}_i - \mathbf{x}) = 0 \quad \forall\, \mathbf{x} \in \mathcal{P}, \forall\, i \in [1..n]. \quad (4)$$

Provided that all $h_i(\mathbf{x})$ are $\mathcal{C}^k$, non-negative, and with a non-vanishing sum inside $\mathcal{P}$, barycentric coordinates satisfying conditions (a)–(d) can be constructed via direct normalization:

$$\lambda_i(\mathbf{x}) = h_i(\mathbf{x}) / \sum_{k=1..n} h_k(\mathbf{x}). \quad (5)$$

Orthogonal duals. Now let $\mathbf{x}$ be an arbitrary point inside $\mathcal{P}$. Define a set of vectors $\mathbf{n}_i(\mathbf{x}) = (\mathbf{v}_i - \mathbf{x})/|\mathbf{v}_i - \mathbf{x}|$. For a set of homogeneous coordinates, these vectors satisfy, by construction,

$$\sum_{i=1..n} h_i(\mathbf{x})|\mathbf{v}_i - \mathbf{x}|\ \mathbf{n}_i(\mathbf{x}) \overset{\text{Eq. (4)}}{=} 0.$$

This relation directly implies, through Minkowski's theorem [Klain 2004], the existence of a unique (up to translation) *convex polytope* $\mathcal{D}(\mathbf{x})$ in $\mathbb{R}^d$, of which the face normals are given by the unit vectors $\mathbf{n}_i(\mathbf{x})$ and the corresponding face areas are $h_i(\mathbf{x})|\mathbf{v}_i - \mathbf{x}|$. By construction, such a polytope is *orthogonally dual* to the triangulation $\mathcal{T}$ of points $\{\mathbf{x}\} \cup \{\mathbf{v}_i\}_{i=1..n}$ with $\mathbf{x}$ and $\mathbf{v}_i$ connected iff $h_i(\mathbf{x}) > 0$. This argument was already made in [Langer et al. 2006], but was not exploited to parameterize extended coordinates through power diagrams. We also note the similarity of this argument with the Maxwell-Cremona equivalence of self-supporting structures with 2D power diagrams used in [de Goes et al. 2013].

Conversely, given any convex polytope $\mathcal{D}(\mathbf{x})$ such that each facet f_i (with normal $\mathbf{n}_i$ and area $|f_i|$) is orthogonal to $(\mathbf{v}_i - \mathbf{x})$, we have:

$$0 = \int_{\mathcal{D}(\mathbf{x})} \mathbf{n}(s) ds = \sum_{i=1..n} \mathbf{n}_i |f_i| = \sum_{i=1..n} \frac{|f_i|}{|\mathbf{v}_i - \mathbf{x}|} (\mathbf{v}_i - \mathbf{x}).$$

Therefore, based on Eq. (4), the n functions

$$h_i(\mathbf{x}) = |f_i| / |\mathbf{v}_i - \mathbf{x}| \quad (6)$$

define homogeneous, non-negative coordinates. Their sum is also guaranteed not to vanish provided that $\mathcal{D}(\mathbf{x})$ is not degenerate (i.e., not reduced to a point). The geometry of $\mathcal{D}(\mathbf{x})$ then defines generalized barycentric coordinates.

Geometric equivalence. We conclude that there is a *one-to-one* correspondence between non-negative homogeneous coordinates at any interior point $\mathbf{x} \in \mathcal{P}$ and orthogonal dual cells. This implies that we can parameterize the set of *all generalized barycentric coordinates* satisfying conditions (a)–(c) over a convex polytope $\mathcal{P}$ by the power weights as functions of $\mathbf{x}$. One can see this parameterization as a geometric counterpart to the analytical parameterization of [Floater et al. 2006] (we will make this link more formal in Sec. 3.4), which now generalizes to arbitrary dimensions.

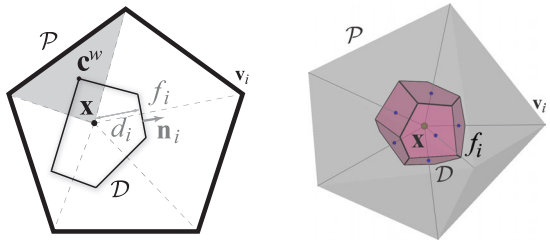

Figure 1: ***Power coordinates.*** *From a set of weights on the vertices $\mathbf{v}_i$ of a polygon (left) or polytope (right) $\mathcal{P}$, the power cell of a point $\mathbf{x}$ (with weight 0) offers a simple geometric interpretation of continuous, non-negative linearly-precise barycentric coordinates.*

2.3 From power diagrams to coordinates

Our geometric characterization of generalized barycentric coordinates suggests a simple approach to both formulate *and* evaluate barycentric coordinates, which turns out to be linked to the notion of discrete Hodge stars on meshes.

Power coordinates evaluation. We can now explicitly describe how a convex polytope $\mathcal{P}$ and a given choice of weights $w_i(\mathbf{x})$ can be used to compute exactly the corresponding coordinates. For a point $\mathbf{x}$ inside $\mathcal{P}$, we proceed as follows to evaluate the power barycentric coordinates $\lambda_i(\mathbf{x})$:

1. From the n vertices $\mathbf{v}_1, ..., \mathbf{v}_n$ of polytope $\mathcal{P}$, create $(n+1)$ weighted points: $(\mathbf{v}_1, w_1(\mathbf{x})), ..., (\mathbf{v}_n, w_n(\mathbf{x}))$, to which we add $(\mathbf{x}, 0)$, *i.e.*, the evaluation point with a weight of zero.
2. Compute the power diagram of these $(n+1)$ weighted points, which generates a power cell $\mathcal{D}$ associated to point $\mathbf{x}$.
3. Compute the homogenous coordinates h_i as follows: if the edge from $\mathbf{x}$ to $\mathbf{v}_i$ is present in the regular triangulation dual

to the power diagram, set: $h_i = |f_i|/|\mathbf{x}-\mathbf{v}_i|$, where f_i is the facet of $\mathcal{D}$ dual to the edge; otherwise, set $h_i = 0$.

4. Normalize the homogeneous coordinates via Eq. (5) to obtain the power coordinates λ_i at $\mathbf{x}$.

Note that we assigned a weight of 0 to the evaluation point $\mathbf{x}$ for simplicity: weights being defined up to a constant (see Sec. 2.1), this choice has no bearing on the generality of our approach.

Implementation. The power diagram construction and the areas and lengths involved in the evaluation of the coordinates are trivially handled via the use of a computational geometry library such as CGAL [CGAL 2016]: one simply needs to use the class `Regular_triangulation_3`, and insert – possibly in parallel for efficiency – the n+1 weighted points (see Supplemental Material for code), before reading off the geometric quantities from the resulting power diagram. For an n-vertex polytope, constructing the power diagram costs $\mathcal{O}(n \log n)$ in 2D, and $\mathcal{O}(n^{\lceil d/2 \rceil})$ in dD for $d > 2$. Power coordinates are thus very easy and efficient to compute for the typically small values of n used in practice. Finally, this construction still holds on facets of $\mathcal{P}$, where the dual polytope $\mathcal{D}$ is now unbounded in the normal direction of the facet—but all previous expressions remain valid in this limit case. This implies that evaluations of barycentric coordinates near the boundary are very stable if a robust library is used to compute power diagrams. Otherwise, a simple distance thresholding approach can be implemented to avoid numerical degeneracies.

Coordinates as Hodge stars. Suppose we pick a point $\mathbf{x} \in \mathcal{P}$, for which we construct the dual orthogonal cell $\mathcal{D}(\mathbf{x})$ corresponding to a given choice of weights (we will provide concrete examples of weights shortly). Note that the homogeneous coordinates—and thus, the barycentric coordinates up to normalization—are expressed as a ratio of volume of dual facets of the power cell $\mathcal{D}(\mathbf{x})$ and volume of their associated primal edges, see Eq. (6). In Discrete Exterior Calculus (DEC [Desbrun et al. 2008]), this expression corresponds to the edge-based *Hodge star* $\star_1$ for 1-forms, as

$$\star_1 = \mathrm{diag}(h_i).$$

This connection becomes obvious if one notices that Eq. (4) can be reexpressed in the DEC formalism through:

$$d_0^t \ \star_1 d_0 \ \mathbf{X} = 0,$$

where $\mathbf{X}$ is seen as a 0-form denoting the coordinates of the vertices and the evaluation point, and d_0 is the exterior derivative corresponding to a signed adjacency matrix. Linear precision of coordinates thus amounts to what was referred in [Glickenstein 2005; de Goes et al. 2014b] as the *linear precision of the generalized Laplacian operator* when using weighted diagonal Hodge stars.

2.4 Existence condition

Due to gauge invariance, we saw in Sec. 2.3 that we can always fix the weight for the evaluation point $\mathbf{x}$ to 0 without loss of generality. However, arbitrary assignment of other weights may not always lead to useful coordinates: given an arbitrary set of weighted points, the power cell associated with the evaluation location $\mathbf{x}$ may become empty. Weights must thus be chosen such that the power cell $\mathcal{D}(\mathbf{x})$ corresponding to the weighted point $(\mathbf{x}, 0)$ is non-degenerate for any $\mathbf{x} \in \mathcal{P}$. Thankfully, this is a simple condition to enforce.

Theorem. *For a point $\mathbf{x}$, the power cell $\mathcal{D}(\mathbf{x})$ is not degenerate if and only if there is a vector $\mathbf{t} \in \mathbb{R}^d$, such that*

$$|\mathbf{v}_i - \mathbf{x}|^2 - w_i(\mathbf{x}) + \mathbf{t} \cdot (\mathbf{v}_i - \mathbf{x}) \geq 0 \ \ \forall i = 1 \dots n, \qquad (7)$$

with the inequality being strict for at least one of them.

Proof: By adding a linear function to the weight (see Sec. 2.1), we can always translate the dual polytope $\mathcal{D}(\mathbf{x})$ by a vector $\mathbf{t}(\mathbf{x})$ in order for point $\mathbf{x}$ to be inside $\mathcal{D}(\mathbf{x})$. Then the cell is not degenerate (i.e., not empty) if and only if the signed distances from $\mathbf{x}$ to the faces of this shifted dual along the corresponding primal edges are all non-negative, with at least one of them being strictly positive: this results from Eq. (2), which is now rewritten using the distance d_i between $\mathbf{x}$ and the power cell facet dual to edge $\mathbf{v}_i\mathbf{x}$ through

$$d_i = \frac{|\mathbf{v}_i - \mathbf{x}|^2 - w_i(\mathbf{x})}{2|\mathbf{v}_i - \mathbf{x}|}. \qquad (8)$$

■

As a corollary of Eq. (7), a trivial sufficient condition for non-degeneracy of the power cell is thus

$$w_i(\mathbf{x}) \leq |\mathbf{v}_i - \mathbf{x}|^2. \qquad (9)$$

Note that this happens to be the same condition as in [de Goes et al. 2014b] in the very different context of generalizing orthogonal dual cells on non-flat triangle meshes through weights.

2.5 Properties

If the non-degeneracy condition is enforced, power coordinates have —or can easily be made to have— valuable properties beyond linear precision:

- **Non-negativity.** Since the homogeneous power coordinates are non-negative by construction, the condition of non-degeneracy discussed above also enforces that the denominator of Eq. (5) can never be zero. As a result, power barycentric coordinates are well-defined and non-negative anywhere in $\mathcal{P}$.
- **Locality.** The cells of some vertices of $\mathcal{P}$ may not share a dual facet with the cell of $\mathbf{x}$, thus resulting in zero coordinates. Our construction can thus seamlessly offer *local* coordinates as proposed in [Zhang et al. 2014]. Indeed, depending on the choice of weight functions, the evaluation point $\mathbf{x}$ can be far enough away from a given vertex $\mathbf{v}_i$ that they no longer share a dual facet in the power diagram. The vertex $\mathbf{v}_i$ then loses its influence on $\mathbf{x}$ since the corresponding λ_i vanishes.
- **Similarity invariance.** Invariance of coordinates to rotation, translation, and scaling of the polytope $\mathcal{P}$ is often desirable. Here again, we can easily accommodate these requirements. Power barycentric coordinates are rotation and translation invariant if the weights themselves are—an example being weights that are functions of geometric measures like distances or volumes. They will also be invariant under scaling of $\mathcal{P}$ by a factor of s iff the pointwise duals $\mathcal{D}(\mathbf{x})$ get uniformly scaled as well. This can be easily achieved by making sure that the input weights are of SI unit $[m^2]$ through normalization by the proper power of the volume of the polytope (or any other geometric measure). We will provide entire families of such coordinates in Sec. 4.
- **Continuity.** As can be seen from Eq. (3), a power cell $\mathcal{D}(\mathbf{x})$ (and its face areas in particular) are smoothly dependent on the weights. Therefore, by choosing continuous weight functions $w_i(\mathbf{x})$ we automatically inherit continuity for the corresponding power coordinates.

2.6 Smoothness

Smoothness of our coordinates deserves a closer inspection as it is the least trivial property to obtain in our framework. We first define a reference connectivity which will allow us to express a sufficient condition of smoothness—and a systematic approach to render C^∞ the power coordinates derived from an arbitrary set of weights.

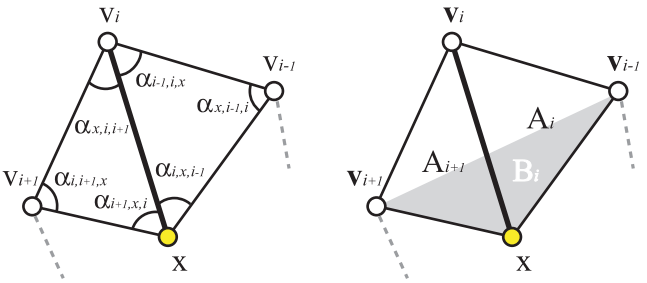

Figure 2: ***Conventions*** *for Eq. (10) and Eq. (13), respectively.*

Full-connectivity homogenous coordinates. Until now, we always derived the connectivity of the power diagram (and of its dual triangulation) based on the weights at vertices of $\mathcal{P}$ and on the position of the evaluation point $\mathbf{x}$. However, it is common practice to define an imposed connectivity for the triangulation, and express a *weighted circumcentric dual* $\mathcal{W}(\mathbf{x})$ for which weights are used to derive a weighted circumcenter $\mathbf{c}_\sigma^w$ per simplex σ of this triangulation that are then connected into the dual $\mathcal{W}$ based on the adjacency between simplices: this is what was proposed in [de Goes et al. 2014b] for instance, for a given triangle mesh with a weight per vertex. The weighted circumcentric dual $\mathcal{W}(\mathbf{x})$ is not necessarily embedded: flips of edges and faces are possible (see inset: red face f_i is flipped; for these weights, the power cell $\mathcal{D}$ would be the black convex cell, but the weighted circumcentric dual $\mathcal{W}$ is, instead, the polygon including the fish tail shape). In our context, we define a "full-connectivity" triangulation of $\mathcal{P} \bigcup \mathbf{x}$ to be the triangulation formed by $\mathcal{P}$ (after its facets are triangulated) and all the edges linking $\mathbf{x}$ to the vertices $\mathbf{v}_i$ of $\mathcal{P}$. This triangulation, along with the weights $w_i(\mathbf{x})$ (and 0 for $\mathbf{x}$), induces a Hodge star $H_i^w(\mathbf{x})$ per edge $\mathbf{x}\mathbf{v}_i$, for which an explicit formulation in 2D reads [Mullen et al. 2011]

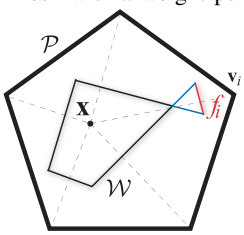

$$H_i^w(\mathbf{x}) = \frac{1}{2}(\cot\alpha_{i,i+1,x} + \cot\alpha_{x,i-1,i}) \qquad (10)$$
$$+ \frac{\cot\alpha_{i+1,x,i}}{2|\mathbf{x}-\mathbf{v}_i|^2}(w_i(\mathbf{x}) - w_{i+1}(\mathbf{x})) - \frac{\cot\alpha_{x,i,i+1}}{2|\mathbf{x}-\mathbf{v}_i|^2}w_{i+1}(\mathbf{x})$$
$$+ \frac{\cot\alpha_{i,x,i-1}}{2|\mathbf{x}-\mathbf{v}_i|^2}(w_i(\mathbf{x}) - w_{i-1}(\mathbf{x})) - \frac{\cot\alpha_{i-1,i,x}}{2|\mathbf{x}-\mathbf{v}_i|^2}w_{i-1}(\mathbf{x}),$$

where $\alpha_{i,x,i-1}$ is the angle at $\mathbf{x}$ in the triangle $(\mathbf{x}, \mathbf{v}_{i-1}, \mathbf{v}_i)$ as described in Fig. 2(left). The 3D version $H_i^w(\cdot)$ can be similarly assembled from the weighted circumcenters computed from Eq. (3). These Hodge star values H_i^w still form homogeneous coordinates in the sense of Eq. (4), but they are *not necessarily* satisfying positivity. We refer to these star values as the *full-connectivity homogeneous coordinates*.

Smoothness condition. Now that we have introduced the Hodge star edge values computed from the triangulation with full connectivity, we can express a sufficient condition for C^∞ of our power coordinates $\lambda_i(\mathbf{x})$.

Lemma. *The power coordinates derived from weights $w_i(\mathbf{x})$ are C^∞ if the weight functions $w_i(\mathbf{x})$ are also C^∞, and if*

$$H_i^w(\mathbf{x}) \geq 0 \quad \forall i = 1..n. \qquad (11)$$

Proof: Positivity of the full-connectivity homogeneous coordinates H_i^w for all $\mathbf{x}$ readily implies that the edge $\mathbf{x}\mathbf{v}_i$ is part of the regular triangulation induced by the power diagram of the weighted vertices $(\mathbf{v}_i, w_i)$ of $\mathcal{P}$ and $(\mathbf{x}, 0)$ [Glickenstein 2005] Now, if every $w_i(\cdot)$ is C^∞ and since the regular triangulation dual to the power diagram keeps the same connectivity for all $\mathbf{x}$, the power coordinates are C^∞ because the signed dual facet volumes are C^∞ functions of $\mathbf{x}$: only a change of connectivity in the power diagram could induce a loss of smoothness. ■

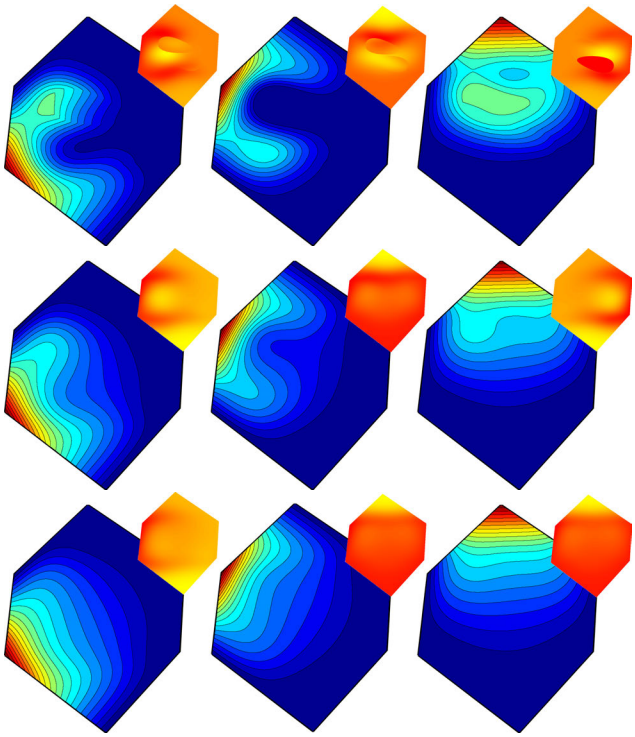

Figure 3: ***Increasing smoothness.*** *From an original C^0 coordinates (top) with discontinuous derivatives (inset: y-component of gradient in orange hues), we can turn them into C^∞ coordinates by computing the weight shift M described in Sec. 2.6, or using an even larger shift (bottom), which smooths the basis functions.*

Smoothness correction. While the condition above is only sufficient, we can derive from it a procedure to render any set of weights C^∞: we can always shift them by a constant to meet the condition $H_i^w(\mathbf{x}) \geq 0 \ \forall i$. Indeed, for a given d-dimensional polytope $\mathcal{P}$ and a set of weights, define:

$$M = \max\left\{0, \ -\inf_{\mathbf{x},i} \frac{H_i^w(\mathbf{x}) \ |\mathbf{x}-\mathbf{v}_i|^d}{s_i(\mathbf{x})}\right\},$$

where $s_i(\mathbf{x})$ equals the volume of the $(d-1)-$dimensional face associated with $\mathbf{v}_i$ of the Wachspress dual of $\mathcal{P}$ times $|\mathbf{x}-\mathbf{v}_i|^{d-1}$. M is finite because the unitless denominator s_i is bounded away from zero: it is the volume (length when $d=2$, area when $d=3$) of the stereographic projection along $\mathbf{x}\mathbf{v}_i$ of the spherical $(d-1)-$polygon formed by the unit normals of the faces incident to $\mathbf{v}_i$—which has a minimum of κ_i, the Gaussian curvature at vertex i, assumed to be strictly positive (see Sec. 1.1). In practice, we can find an evaluation of M by either sampling the interior of $\mathcal{P}$ in a preprocessing phase, or using a less tight but safe upper bound, such as $\inf_i(H_i^w/\kappa_i) \cdot diam(\mathcal{P})^d$, where $diam$ is the diameter operator, i.e., the maximum distance between pairs of vertices. Then, assuming similarity invariance is enforced (see Sec. 2.5), the SI unit of M is $[m^{2d-2}]$; consequently, the use of altered weights $\tilde{w}_i$ defined as:

$$\tilde{w}_i(\mathbf{x}) = w_i(\mathbf{x}) - M^{1/(d-1)},$$

is guaranteed to lead to smooth coordinates as their corresponding full-connectivity homogeneous coordinates $H_i^{\tilde{w}}$ are non-negative. Note that the weight at $\mathbf{x}$ is kept fixed at 0, and M depends on

the polygon shape; but the resulting λ_i is similarity invariant. This shift by M can be understood as a blend of the (non-smooth) power coordinates with the always-smooth Wachspress coordinates.

While highly application-dependent, the design of smooth, positive, and linear-precise coordinates is thus rather simple, as it only requires a few conditions on weights to guarantee relevance of the resulting power coordinates. We provide a number of examples in Sec. 4, after discussing the geometric interpretation of existing barycentric coordinates in our framework.

3 Existing Power Coordinates

Before formulating new weights, we review existing coordinates for convex polytopes to show that they correspond in our power coordinates framework to very simple choices of weights, providing straightforward extensions to arbitrary dimensions.

3.1 Wachspress coordinates

Ju et al. [2005a] noticed that Wachspress coordinates can be expressed in terms of the polar dual of the input polytope $\mathcal{P}$, i.e., using a dual cell $\mathcal{D}(\mathbf{x})$ for which the distance from $\mathbf{x}$ to a dual face f_i is $d_i = 1/|\mathbf{v}_i - \mathbf{x}|$. This is, in fact, a particular case of our generalized notion of dual, and using Eq. (2) we directly conclude that Wachspress coordinates are expressed in arbitrary dimensions as:

$$w_i^{\text{Wach}}(\mathbf{x}) = |\mathbf{x} - \mathbf{v}_i|^2 - 2.$$

Note that the constant 2 can be changed to any strictly positive constant: normalization (Eq. (5)) will lead to the same coordinates.

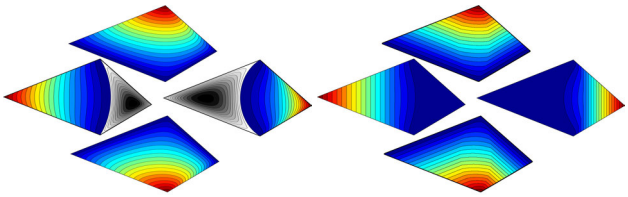

Figure 4: ***Discrete harmonic coordinates.*** *While the original discrete harmonic coordinates (left) can go negative (grey colors) in convex polygons, our power variant (right) remain positive (rainbow colors) everywhere by construction, but may only be C^0.*

3.2 Power discrete harmonic

Discrete Harmonic coordinates [Meyer et al. 2002] are also trivially related to a notion of dual, as they are the coordinates corresponding to the canonical, circumcenter-based Hodge star. Thus, they correspond to the case where $\mathcal{D}(\mathbf{x})$ is the classical Voronoi cell of $\mathbf{x}$, hence to *zero weights*. In 3D, these null weights correspond to the coordinates dubbed "Voronoi" in [Ju et al. 2007]. However, our power diagram construction guarantees non-negativity, they are thus more directly related to the Laplace coordinates defined in [Hiyoshi and Sugihara 1999]. The power form of discrete harmonic coordinates are in general *not* smooth, only continuous, see Fig. 4. However, note that this variant is quite different from a simple thresholding of the discrete harmonic homogeneous coordinates: instead, our power coordinates are linear precise, a property that simply discarding negative homogeneous coordinates (i.e., thresholding them to zero) would not enforce.

3.3 Mean value coordinates: old and new

The initial derivation of mean value coordinates by Floater [2003] relies on the local integration of the normal of a unit circle centered at $\mathbf{x}$. While this seems unrelated to the polytopal dual cell that our construction relies on, one realizes that in fact, creating a cell $\mathcal{D}(\mathbf{x})$ such that each distance d_i from $\mathbf{x}$ to a facet f_i of $\mathcal{D}(\mathbf{x})$ is *unit* (or, more generally, constant) leads to the exact same normal integral as in the original derivation. This particular dual (see inset) is thus *circumscribing* the unit circle, and using Eq. (2) once again, we find that the weights needed to exactly reproduce mean value coordinates are:

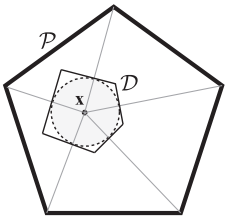

$$w_i^{\text{MVC}}(\mathbf{x}) = |\mathbf{v}_i - \mathbf{x}|^2 - 2|\mathbf{v}_i - \mathbf{x}|. \tag{12}$$

Again, the factor 2 can be replaced by any strictly positive constant without affecting the normalized coordinates.

Somehow surprisingly, this orthogonal dual construction with unit distances d_i leads in 3D to a very different set of coordinates: while the existing 3D extension of MVC [Ju et al. 2005b; Floater et al. 2005] relies on barycentric coordinates over spherical triangles, our homogeneous coordinates are still ratios of volumes of a straight-edge dual cell that circumscribes the unit sphere. As a consequence, the power variant happens to be significantly less distorted as demonstrated in Figs. 5 and 6. Moreover, our construction generalizes to higher dimensions in a straightforward manner since the expression of w_i^{MVC} above still holds as is.

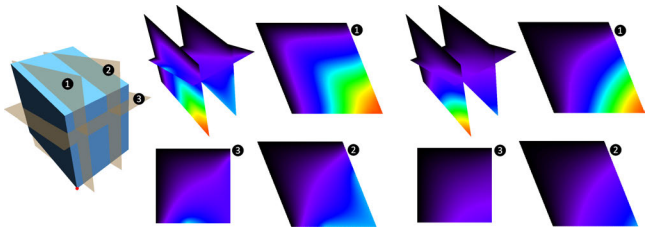

Figure 5: ***Original vs. Power Mean Value Coordinates.*** *Even on a simple parallelepiped (left), the original MVC [Ju et al. 2005b] (center) for the bottom-right corner marked with a red dot exhibits a more asymmetric behavior than our power variant (right).*

3.4 3-point and 5-point coordinates in 2D

Floater et al. [Floater et al. 2006] introduced a general parameterization of barycentric coordinates by smooth functions c_i through the following homogenous expressions:

$$h_i = \frac{c_{i+1}A_{i-1} - c_i B_i + c_{i-1}A_i}{4A_i A_{i-1}}, \tag{13}$$

where A_i and B_i are the signed areas of triangles $(\mathbf{x}, \mathbf{v}_i, \mathbf{v}_{i+1})$ and $(\mathbf{x}, \mathbf{v}_{i-1}, \mathbf{v}_{i+1})$ respectively, see Fig. 2(right). Assume that for a given $\mathbf{x}$, the regular triangulation deriving from our power coordinates include the edges $\mathbf{x}\mathbf{v}_i$; then starting from the expression of the canonical weighted Hodge star given in Eq. (10), basic trigonometry leads to weights of the form:

$$w_i(\mathbf{x}) = |\mathbf{x} - \mathbf{v}_i|^2 - c_i(\mathbf{x}), \tag{14}$$

providing a simple geometric interpretation of c_i which extends to arbitrary dimensions. Note that this is not an exact equivalence: our corresponding power coordinates are guaranteed to be positive, while the original parameterization of [Floater et al. 2006] does not: as in the discrete harmonic case, our parameterization is not just a thresholding of the original homogeneous coordinates since it always enforces linear precision, which naive thresholding loses.

Three-point coordinates. Based on the relationship between their parameterization and ours, the explicit weight expressions of

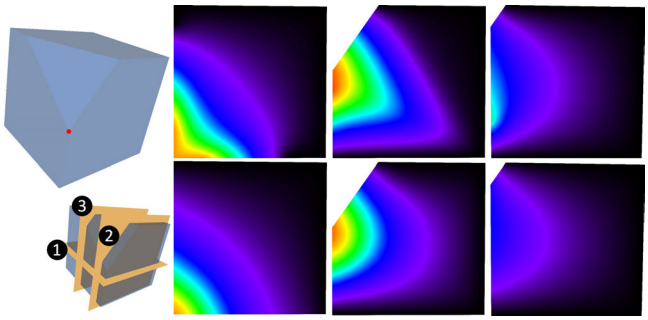

Figure 6: ***3D mean values.*** *For a 3D polytope with 7 faces (left), the mean value coordinates defined in [Ju et al. 2005b] (top) are significantly more distorted than our 3D mean value coordinates (bottom) for the point indicated by the red sphere. Three slices are shown with the order indicated: one horizontal, and two verticals.*

their three-point family are simply, for $\mu \in [0,1]$:

$$w_i^{\mu,1}(\mathbf{x}) = |\mathbf{x}-\mathbf{v}_i|^2 - |\mathbf{x}-\mathbf{v}_i|^{\mu}.$$

Only two cases in this family ($\mu = 0$ and $\mu = 1$) were producing non-negative homogenous coordinates in their formulation; ours enforce non-negativity for all μ instead, at the cost of smoothness: for $\mu \in]0,1[$, the resulting coordinates are only C^0.

Five-point coordinates. Similarly, the expressions for the 5-point Wachspress family and the two types of 5-point mean value family are (for $\mu \in [0,1]$ and where angles are denoted using the conventions depicted in Fig. 2):

$$w_i^{\mu,2}(\mathbf{x}) = |\mathbf{x}-\mathbf{v}_i|^2 - (1+\mu\frac{A_{i-1}+A_i-B_i}{A_{i-1}+A_i}),$$

$$w_i^{\mu,3}(\mathbf{x}) = |\mathbf{x}-\mathbf{v}_i|^2 - |\mathbf{x}-\mathbf{v}_i|\frac{(1+\mu)(\sin\alpha_{i,x,i-1}+\sin\alpha_{i+1,x,i})}{\sin\alpha_{i,x,i-1}+\sin\alpha_{i+1,x,i}+\mu\sin(\alpha_{i+1,x,i-1})},$$

$$w_i^{\mu,4}(\mathbf{x}) = |\mathbf{x}-\mathbf{v}_i|^2 - |\mathbf{x}-\mathbf{v}_i|\frac{\cos(\mu(\alpha_{i,x,i-1}-\alpha_{i+1,x,i}/4))}{\cos(\mu(\alpha_{i,x,i-1}+\alpha_{i+1,x,i}/4))}.$$

4 Other Examples of Power Coordinates

We provide next a series of new coordinates with varying degrees of smoothness, to illustrate the generality of power coordinates.

4.1 Simple power coordinates

One can introduce simple coordinates by simply choosing weights functions w_i that are negative (to trivially enforce the sufficient condition in Eq. (9)) and translation invariant homogeneous functions of $\mathbf{x} \cup \{\mathbf{v}_i\}_{i=1..n}$ of degree 2 (to enforce similarity invariance): they will directly enforce all the conditions (a)–(f), although with C^0 continuity in general. One can also use weights of the form $w_i(\mathbf{x}) = |\mathbf{v}_i - \mathbf{x}|^2 - \hat{w}_i(\mathbf{x})$ for any $\hat{w}_i$'s that are non-negative translation invariant homogeneous functions of $\mathbf{x} \cup \{\mathbf{v}_i\}_{i=1..n}$ of arbitrary degree. Scale invariance is easy to enforce through the proper choice of exponent or through normalization by the volume, surface area, or mean-width of the polytope $\mathcal{P}$, as discussed in Sec. 2.5. Moreover, weights that are functions of edge distances such as the ones used in [Malsch and Dasgupta 2004] and their trivial extension using facet distances can also be employed, offering a direct generalization of their results to 3D. Furthermore, should such power coordinates need to be C^∞, the procedure described in Sec. 2.6 can be directly used to ensure smoothness on any given polytope $\mathcal{P}$.

4.2 Mean-Wachspress coordinates

A 2-parameter family of weights that blends Wachspress and mean value coordinates can be trivially formulated as well: for any strictly positive values a and b, weight functions defined as:

$$w_i^{\mathrm{MW}}(\mathbf{x}) = |\mathbf{v}_i - \mathbf{x}|^2 - a - b\,|\mathbf{x}-\mathbf{v}_i|/|\mathcal{P}|^{1/d}, \qquad (15)$$

will induce power coordinates, where the volume $|\mathcal{P}|$ of $\mathcal{P}$ is raised to the inverse of the dimension to enforce similarity invariance. These weights always produce C^∞ coordinates: since they are formed as a combination of Wachspress and mean-value homogeneous coordinates that are strictly positive inside $\mathcal{P}$: thus, the sufficient condition of smoothness discussed in Sec. 2.6 is guaranteed to hold. Fig. 7 illustrates a few of these coordinates in 2D.

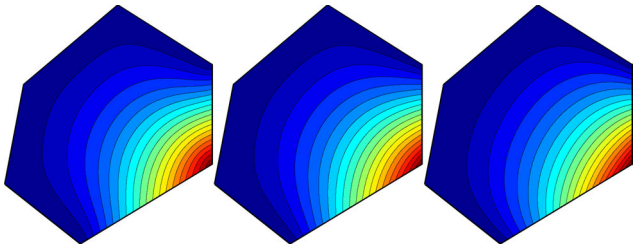

Figure 7: ***Mean-Wachspress.*** *Using the unified expression in Eq. (15), we recover mean value coordinates (left), Wachspress coordinates (right), or a blend between the two (middle).*

4.3 Anisotropic power coordinates

While all the choices of weights presented so far used Euclidean geometric measures such as distances or areas, they can be easily extended to incorporate anisotropy through a norm defined by $|\mathbf{v}|_g^2 = \mathbf{v}^T G \mathbf{v}$ for a constant, symmetric positive definite matrix G. This anisotropic norm allows us to tailor our barycentric coordinates quite directly by substituting the Euclidean norm $|\cdot|$ by $|\cdot|_g$ in previous formulas. In particular, weights of the form $w_i(\mathbf{x}) = |\mathbf{v}_i - \mathbf{x}|^2 - \hat{w}_i(\mathbf{x})$ induce anisotropic barycentric coordinates while staying similarity invariant if the distances used in $\hat{w}_i(\mathbf{x})$'s are modified to be anisotropic. Note that this treatment is reminiscent of the creation of anisotropic Hodge stars (i.e., [de Goes et al. 2014a]) due to the interpretation of coordinates as Hodge star values mentioned in Sec. 2.3.

Anisotropic mean value coordinates. The anisotropic variant of mean value coordinates is particularly interesting, as it has a nice geometric interpretation. Indeed, we define its weights as:

$$w_i^{\mathrm{AMVC}}(\mathbf{x}) = |\mathbf{v}_i - \mathbf{x}|^2 - 2|\mathbf{v}_i - \mathbf{x}|_g. \qquad (16)$$

(Notice that unlike Eq. (15), there is no need to divide by the volume of $\mathcal{P}$: similarity invariance is automatically enforced by the normalization step.) Based on Eq. (2), the distance from the evaluation point $\mathbf{x}$ to the facet of $\mathcal{D}(\mathbf{x})$ that is dual to edge $\mathbf{x}\mathbf{v}_i$ is:

$$d_i = \frac{|\mathbf{v}_i - \mathbf{x}|_g}{|\mathbf{v}_i - \mathbf{x}|}$$

We claim that this particular set of distances d_i can be geometrically constructed as follows. For a given evaluation point $\mathbf{x}$, construct a secondary polytope $\mathcal{Z}$ with vertices $\mathbf{z}_i$ that are at the intersection of the rays $\mathbf{x}\mathbf{v}_i$ and the ellipsoid defined by the set of points $\mathbf{y}$ such that $(\mathbf{y}-\mathbf{x})^t G(\mathbf{y}-\mathbf{x}) = 1$. The new polytope is trivially convex, and the new vertices $\mathbf{z}_i$ are expressed as

$$\mathbf{z}_i - \mathbf{x} = \frac{\mathbf{v}_i - \mathbf{x}}{|\mathbf{v}_i - \mathbf{x}|_g}.$$

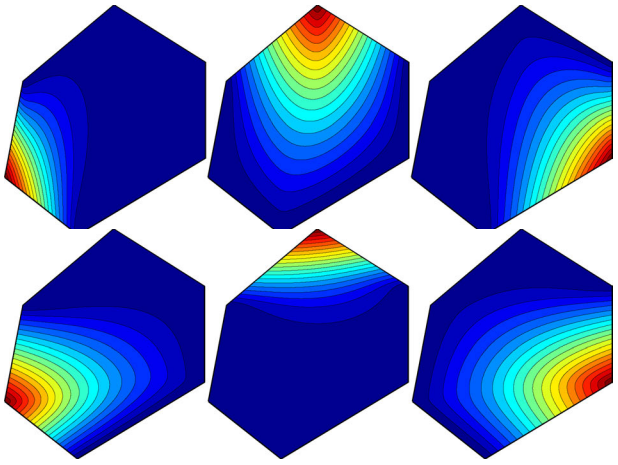

Figure 8: ***Anisotropic 2D mean value coordinates.*** *Computing the mean value weights using a constant metric $G = \mathrm{diag}(15, 1)$ (top) or $G = \mathrm{diag}(1, 15)$ (bottom) generates anisotropic variants of the original mean value coordinates, still satisfying the same properties but with deformed shape functions (see Fig. 7(right)).*

Now consider the *polar dual* of $\mathcal{Z}$ w.r.t. a unit sphere centered at $\mathbf{x}$ and denote the vertices of that polar dual by $\mathbf{p}_i$. One realizes that

$$\mathbf{p}_i - \mathbf{x} = \frac{|\mathbf{v}_i - \mathbf{x}|_g}{|\mathbf{v}_i - \mathbf{x}|^2}(\mathbf{v}_i - \mathbf{x}),$$

and thus $|\mathbf{p}_i - \mathbf{x}| = d_i$. We conclude two things from this observation: first, the dual cell $\mathcal{D}(\mathbf{x})$ is always n-faceted since it corresponds to Wachspress homogeneous coordinates for the polytope $\mathcal{Z}$; second, since $\mathcal{Z}$ depends smoothly on $\mathbf{x}$, these anisotropic mean value coordinates are always C^∞, see Fig. 8. The SPD matrix G defining the norm $|.|_g$ can also be *spatially varying*, i.e., a different matrix for the evaluation of w_i^{AMVC} at a different $\mathbf{x}$: the construction and resulting properties are unchanged, offering even more degrees of freedom to derive additional coordinates, see Fig. 12 (left).

Anisotropic mean-Wachspress coordinates. By the same reasoning, and because Wachspress coordinates are such that $w_i^{\text{Wach}} - |\mathbf{x} - \mathbf{v}_i|^2$ is constant, the anisotropic variant of mean-Wachspress coordinates are also C^∞, and expressed with weights

$$w_i^{\text{AMW}}(\mathbf{x}) = |\mathbf{v}_i - \mathbf{x}|^2 - a - b\,|\mathbf{v}_i - \mathbf{x}|_g / |\mathcal{P}|^{1/d}. \qquad (17)$$

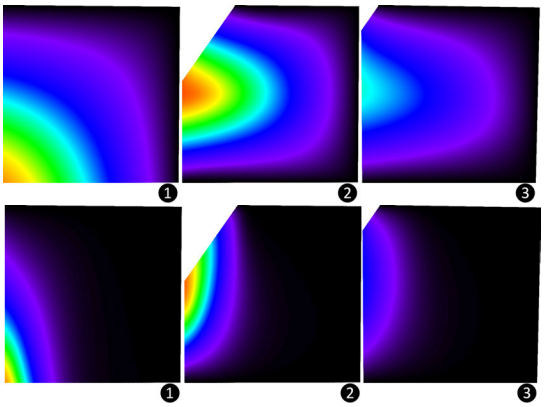

Figure 9: ***Anisotropic 3D mean value coordinates.*** *Using the same polytope and cuts as in Fig. 6, our 3D mean value coordinates for $G = \mathrm{diag}(10, 1, 1)$ (top) and $G = \mathrm{diag}(1, 10, 1)$ (bottom).*

4.4 Iterated power coordinates

Finally, we note that one can even define power coordinates *implicitly* through repeated iterations. For example, for a given evaluation point $\mathbf{x}$ and a convex polytope $\mathcal{P}$, one can compute a *series* of weights $w_i^{(k)}$ (starting with $w_i^{(0)} = w_i^{\text{Wach}}$ for instance) using:

$$w_i^{(k+1)}(\mathbf{x}) = |\mathbf{v}_i - \mathbf{x}|^2 - |\mathbf{v}_i - \mathbf{x}|^{\lambda_i^{(k)}(\mathbf{x})}, \qquad (18)$$

where $\lambda_i^{(k)}(\mathbf{x})$ denotes the power barycentric coordinates derived from weights $w_i^{(k)}$. This procedure converged (in only 3 to 5 iterations) to the same barycentric coordinates for all $w_i^{(0)}$ we chose. The resulting barycentric coordinates (see Figs. 10 and 12(right)) are visually and numerically smooth. While we do not know how to analyze or explicitly formulate the resulting coordinates, note that they come from a repeated "barycentric" averaging of weights, which may allow us to algorithmically define weights in such a way that the resulting coordinates satisfy possibly-intricate implicit relations—maybe even differential relations.

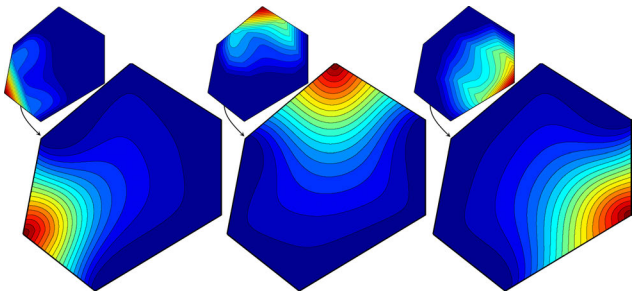

Figure 10: ***Iterated power coordinates.*** *From arbitrary C^0 coordinates (top), 3 iterations of Eq. (18) result in smooth coordinates.*

5 Extensions to Non-Convex Polytopes

The link between homogeneous coordinates and orthogonal duals partially extends to the case of non-convex polygons and polytopes, in particular if we remove the positivity constraint (c).

5.1 Signed coordinates on non-convex 2D polygons

In $\mathbb{R}^2$, there is still a 1-to-1 correspondence between homogeneous coordinates and *weighted circumcentric dual cells* $\mathcal{W}(\mathbf{x})$ described in Sec. 2.6, created as the dual of $\mathbf{x}$ for the simplicial d-manifold with a "full connectivity" linking $\mathbf{x}$ to the vertices of $\mathcal{P}$. Indeed, for any set of functions $h_i(\mathbf{x})$ satisfying Eq. (4), the 2D vectors $\mathbf{f}_i(\mathbf{x}) = h_i(\mathbf{x})(\mathbf{v}_i - \mathbf{x})^\perp$ where $\perp$ denotes a counterclockwise $\pi/2$ rotation, form a closed loop, thus defining the boundary of an orthogonal dual cell $\mathcal{W}(\mathbf{x})$ with possible self-intersections (see inset in Sec. 2.6). The converse is also true: given any orthogonal dual $\mathcal{W}(\mathbf{x})$, $h_i(\mathbf{x})$ defined through the signed diagonal Hodge star would satisfy Eq. (4). Thus, through the weighted circumcentric dual, all homogeneous coordinates h_i have a one-to-one correspondence to an assignment of w_i up to a constant gauge. Note that the homogeneous coordinates can now be negative as a consequence, thus violating condition (c). Replacing the power cell $\mathcal{D}(\mathbf{x})$ by the weighted circumcentric dual $\mathcal{W}(\mathbf{x})$ in our approach recovers the traditional 2D mean value coordinates, which are valid (but often with negative coordinates) on arbitrary polygons.

5.2 Signed coordinates on non-convex 3D polytopes

The 3D case is more involved for two reasons. First, even though there is still a 1-to-1 correspondence between power cells and

non-negative homogeneous coordinates as implied by the work of Memari et al. [2012], the resulting coordinates are not guaranteed to be continuous for continuous weights anymore, thus violating condition (d): the power cell itself can exhibit discontinuous behavior because the visibility vectors connecting $\mathbf{x}$ to vertices $\mathbf{v}_i$ change their relative configuration as the evaluation point moves around a non-convex polytope. Second, if we remove the positivity constraint, the resulting arbitrary homogeneous coordinates are not fully characterized by our weighted circumcentric construction: while Minkowski's theorem guarantees the existence of a convex orthogonally dual polytope from a sequence of (possibly flipped) normals, such a polytope is no longer necessarily a weighted circumcentric dual. As a consequence, a truly general extension of power coordinates for non-convex polytopes remains open. Nevertheless, our weighted circumcentric approach still spans valid homogeneous coordinates that are potentially negative, leading to signed barycentric coordinates if their sums $\sum_i h_i$ are bounded away from zero; e.g., we can recover well-known coordinates such as the Voronoi coordinates in 3D mentioned in [Ju et al. 2005a].

5.3 Positive-power mean value coordinates.

If one still requires true generalized barycentric coordinates satisfying all the conditions (a)-(d), our geometric characterization of coordinates over convex polytopes – in particular, our use of a secondary polytope in Sec. 4.3 – suggests a simple way to extend power coordinates to non-convex polytopes: one can construct a secondary polytope by smoothly displacing the original vertices depending on the evaluation point. We can indeed alter the position of the vertices to make the modified polytope *star-shaped* with respect to the evaluation point; using the mean value weights given in Eq. (12), we can still construct a non-degenerate power cell which will be, by definition, still circumscribed to the unit sphere, but that may involve only a subset of the vertices of the non-convex polytopes. For instance, in order to evaluate positive generalized barycentric coordinates for the evaluation point $\mathbf{x}$ inside the 7-vertex non-convex polygon displayed in the inset, the pink polygon is used. This star-shaped polygon is found by ignoring the obstructed vertex $\mathbf{v}_5$ blocked by the concave vertex $\mathbf{v}_6$, and by displacing vertex $\mathbf{v}_4$ to a modified position $\tilde{\mathbf{v}}_4$ along the edge $\mathbf{v}_3\mathbf{v}_4$.

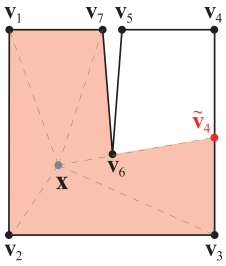

(Note that it corresponds to the visible portion of the polygon used in the positive MVC coordinates [Lipman et al. 2007].) This construction, once the barycentric coefficients are redistributed to the displaced vertices, results in true coordinates, without discontinuity due to visibility as demonstrated in Fig. 11. The ensuing coordinates are thus both local (in the sense advocated in [Zhang et al. 2014]), and positive [Lipman et al. 2007], but require no quadrature to evaluate – making them particularly well suited to cage-based deformation of meshes. We leave implementation details and analysis of this construction in 2D and 3D to a forthcoming paper.

6 Future Work

Our characterization of coordinates based on power duals opens a number of avenues for future work. We mention a few in lieu of a conclusion to illustrate both the current limitations of power coordinates and the opportunities that our work offers.

Theoretical developments. Given the generality of power coordinates, finding necessary conditions on the weights for smoothness, deriving simple and efficient evaluations of their derivatives, or proving contraction for iterated power coordinates are examples of results that could have very practical consequences. The use of power coordinates to define higher-order Whitney basis functions using the work of Gillette et al. [2016] is also of great interest.

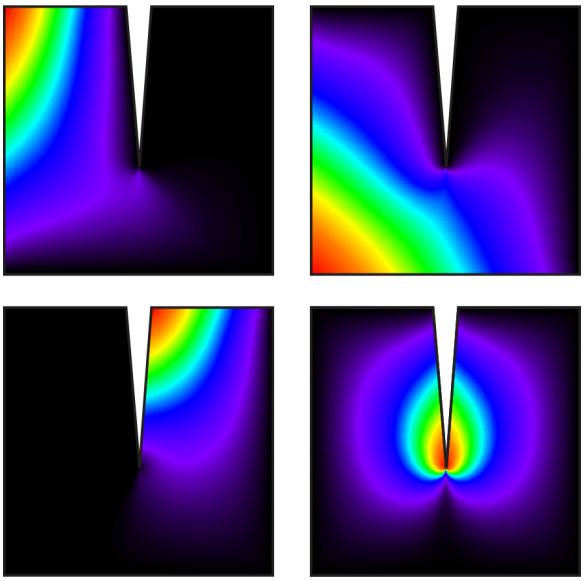

Figure 11: ***Positive Power Mean Value Coordinates.*** *Even on non-convex polytopes, one can use the power mean value coordinates on a "secondary" star-shaped polytope to force positivity. Here, four basis functions are displayed using a rainbow color ramp.*

Harmonic coordinates. Coordinates issued from partial differential equations have not found wide acceptance due to the memory footprint required by the storage of solutions, despite the clear advantage of being positive on arbitrary polygons. A natural question is whether the additional insight afforded by power coordinates can result in an explicit or iterated formulation (see Sec. 4.4) which could be evaluated without the need for precomputed solutions.

Bézier patches. Non-negative barycentric coordinates over polytopes have been shown crucial to offer multisided Bézier patches in [Loop and DeRose 1989], and recently in [Varady et al. 2016]. Rewriting their construction in the context of power coordinates may help in providing fast evaluations of these general patches.

Coordinates on non-convex polytopes. Although we showed how our construction extends naturally to non-convex polytopes, we have only scratched the surface of what can be accomplished for this case. Understanding a general construction with the same efficiency of evaluation is an obvious future work.

Transfinite interpolants. Finally, the notion of power diagram for pointsets extends to continuous power diagrams of curves, which can be computed rather efficiently [Hoff et al. 1999]. Consequently, our construction will converge as a polytope is refined to capture a smooth shape (inset: example of power Voronoi dual for 3D bean shape). This extension is similar to the transfinite form of Sibsons interpolant [Gross and Farin 1999], and closed-form solutions of specific choices of weight functions are possible and could offer valuable new transfinite interpolants as well.

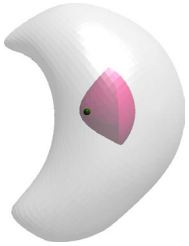

Acknowledgements

We are indebted to Fernando de Goes and the reviewers for their feedback. This work was partially supported through NSF grants CCF-1011944, IIS-0953096, CMMI-1250261 and III-1302285. MD gratefully acknowledges the Inria International Chair program and all the members of the TITANE team for their support as well.

References

ARROYO, M., AND ORTIZ, M. 2006. Local maximum-entropy approximation schemes: a seamless bridge between finite elements and meshfree methods. *Int. J. Num. Meth. Eng. 65*, 13, 2167–2202.

BELYAEV, A. 2006. On transfinite barycentric coordinates. In *Symp. Geo. Processing*, 89–99.

BEN-CHEN, M., WEBER, O., AND GOTSMAN, C. 2009. Variational harmonic maps for space deformation. *ACM Trans. Graph. 28*, 3 (July), Art. 34.

BRUVOLL, S., AND FLOATER, M. S. 2010. Transfinite mean value interpolation in general dimension. *Journal of Computational and Applied Mathematics 233*, 7, 1631–1639.

BUDNINSKIY, M., LIU, B., DE GOES, F., TONG, Y., ALLIEZ, P., AND DESBRUN, M. 2016. Optimal Voronoi tessellations with Hessian-based anisotropy. *ACM Trans. Graph. 36*, 6.

BUSARYEV, O., DEY, T., WANG, H., AND REN, Z. 2012. Animating bubble interactions in a liquid foam. *ACM Trans. Graph. 31*, 4, Art. 63.

CGAL. 2016. *CGAL 4.8 User and Reference Manual*. CGAL Editorial Board, http://www.cgal.org.

CUETO, E., SUKUMAR, N., CALVO, B., MARTÍNEZ, M. A., CEGOÑINO, J., AND DOBLARÉ, M. 2003. Overview and recent advances in natural neighbour Galerkin methods. *Archives of Computational Methods in Engineering 10*, 4, 307–384.

DASGUPTA, G., AND WACHSPRESS, E. L. 2008. Basis functions for concave polygons. *Computers & Mathematics with Applications 56*, 2, 459–468.

DE GOES, F., BREEDEN, K., OSTROMOUKHOV, V., AND DESBRUN, M. 2012. Blue noise through optimal transport. *ACM Trans. Graph. 31*, 6, Art. 171.

DE GOES, F., ALLIEZ, P., OWHADI, H., AND DESBRUN, M. 2013. On the equilibrium of simplicial masonry structures. *ACM Trans. Graph. 32*, 4, Art. 93.

DE GOES, F., LIU, B., BUDNINSKIY, M., TONG, Y., AND DESBRUN, M. 2014. Discrete 2-tensor fields on triangulations. *Comput. Graph. Forum 33*, 5, 13–24.

DE GOES, F., MEMARI, P., MULLEN, P., AND DESBRUN, M. 2014. Weighted triangulations for geometry processing. *ACM Trans. Graph. 33*, 3, Art. 28.

DE GOES, F., WALLEZ, C., HUANG, J., PAVLOV, D., AND DESBRUN, M. 2015. Power particles: An incompressible fluid solver based on power diagrams. *ACM Trans. Graph. 34*, 4, Art. 50.

DESBRUN, M., KANSO, E., AND TONG, Y. 2008. Discrete differential forms for computational modeling. In *Discrete differential geometry*. Birkhäuser Basel, 287–324.

DYKEN, C., AND FLOATER, M. S. 2009. Transfinite mean value interpolation. *CAGD 26*, 117–134.

ECK, M., DEROSE, T., DUCHAMP, T., HOPPE, H., LOUNSBERY, M., AND STUETZLE, W. 1995. Multiresolution analysis of arbitrary meshes. In *Proceedings of ACM SIGGRAPH*, 173–182.

FLOATER, M. S., KÓS, G., AND REIMERS, M. 2005. Mean value coordinates in 3D. *CAGD 22*, 7, 623–631.

FLOATER, M. S., HORMANN, K., AND KÓS, G. 2006. A general construction of barycentric coordinates over convex polygons. *Advances in Computational Mathematics 24*, 1, 311–331.

FLOATER, M. S. 1997. Parametrization and smooth approximation of surface triangulations. *CAGD 14*, 3, 231 – 250.

FLOATER, M. S. 2003. Mean value coordinates. *CAGD 20*, 1, 19–27.

FLOATER, M. S. 2015. Generalized barycentric coordinates and applications. *Acta Numerica 24* (5), 161–214.

GILLETTE, A., RAND, A., AND BAJAJ, C. 2016. Construction of scalar and vector finite element families on polygonal and polyhedral meshes. *Computational Methods in Applied Math 19*.

GLICKENSTEIN, D., 2005. Geometric triangulations and discrete Laplacians on manifolds. arXiv.org:math/0508188.

GROSS, L., AND FARIN, G. 1999. A transfinite form of Sibson's interpolant. *Discrete Applied Mathematics 93*, 1, 33–50.

HIYOSHI, H., AND SUGIHARA, K. 1999. Two generalizations of an interpolant based on Voronoi diagrams. *International Journal of Shape Modeling 05*, 02, 219–231.

HOFF, K. E., KEYSER, J., LIN, M., MANOCHA, D., AND CULVER, T. 1999. Fast computation of generalized Voronoi diagrams using graphics hardware. In *Proceedings of ACM SIGGRAPH*, 277–286.

HORMANN, K., AND FLOATER, M. S. 2006. Mean value coordinates for arbitrary planar polygons. *ACM Trans. Graph. 25*, 4, 1424–1441.

HORMANN, K., AND SUKUMAR, N. 2008. Maximum entropy coordinates for arbitrary polytopes. *Comp. Graph. Forum 27*, 5, 1513–1520.

JACOBSON, A., BARAN, I., POPOVIĆ, J., AND SORKINE, O. 2011. Bounded biharmonic weights for real-time deformation. *ACM Trans. Graph. 30*, 4 (July), Art. 78.

JOSHI, P., MEYER, M., DEROSE, T., GREEN, B., AND SANOCKI, T. 2007. Harmonic coordinates for character articulation. *ACM Trans. Graph. 26*, 3, Art. 71.

JU, T., SCHAEFER, S., WARREN, J., AND DESBRUN, M. 2005. A geometric construction of coordinates for convex polyhedra using polar duals. In *Symp. Geo. Processing*, 181–186.

JU, T., SCHAEFER, S., AND WARREN, J. 2005. Mean value coordinates for closed triangular meshes. *ACM Trans. Graph. 24*, 3, 561–566.

JU, T., LIEPA, P., AND WARREN, J. 2007. A general geometric construction of coordinates in a convex simplicial polytope. *CAGD 24*, 3, 161–178.

KLAIN, D. A. 2004. The Minkowski problem for polytopes. *Advances in Mathematics 185*, 2, 270–288.

LANGER, T., AND SEIDEL, H.-P. 2008. Higher order barycentric coordinates. *Comp. Graph. Forum 27*, 2, 459–466.

LANGER, T., BELYAEV, A., AND SEIDEL, H.-P. 2006. Spherical barycentric coordinates. In *Symp. Geo. Processing*, 81–88.

LI, X.-Y., JU, T., AND HU, S.-M. 2013. Cubic mean value coordinates. *ACM Trans. Graph. 32*, 4 (July), Art. 126.

LIPMAN, Y., KOPF, J., COHEN-OR, D., AND LEVIN, D. 2007. GPU-assisted positive mean value coordinates for mesh deformations. In *Symp. Geo. Processing*, 117–123.

LIPMAN, Y., LEVIN, D., AND COHEN-OR, D. 2008. Green coordinates. *ACM Trans. Graph. 27*, 3, Art. 78.

LIU, Y., HAO, P., SNYDER, J., WANG, W., AND GUO, B. 2013. Computing self-supporting surfaces by regular triangulation. *ACM Trans. Graph. 32*, 4.

LOOP, C. T., AND DEROSE, T. D. 1989. A multisided generalization of Bézier surfaces. *ACM Trans. Graph. 8*, 3, 204–234.

MALSCH, E. A., AND DASGUPTA, G. 2004. Shape functions for polygonal domains with interior nodes. *International Journal for Numerical Methods in Engineering 61*, 8, 1153–1172.

MALSCH, E. A., AND DASGUPTA, G. 2005. Algebraic construction of smooth interpolants on polygonal domains. *The Mathematica Journal 9*, 3, 641–658.

MALSCH, E. A., LIN, J. J., AND DASGUPTA, G. 2005. Smooth two-dimensional interpolations: A recipe for all polygons. *Journal of Graphics, GPU, and Game Tools 10*, 2, 27–39.

MANSON, J., AND SCHAEFER, S. 2010. Moving least squares coordinates. *Comp. Graph. Forum 29*, 5, 1517–1524.

MANSON, J., LI, K., AND SCHAEFER, S. 2011. Positive Gordon-Wixom coordinates. *CAD 43*, 11, 1422–1426.

MEMARI, P., MULLEN, P., AND DESBRUN, M. 2012. Parametrization of generalized primal-dual triangulations. In *International Meshing Roundtable*. 237–253.

MEYER, M., BARR, A., LEE, H., AND DESBRUN, M. 2002. Generalized barycentric coordinates on irregular polygons. *J. Graph. Tools 7*, 1, 13–22.

MILBRADT, P., AND PICK, T. 2008. Polytope finite elements. *Int. J. Num. Meth. Eng. 73*, 12, 1811–1835.

MULLEN, P., MEMARI, P., DE GOES, F., AND DESBRUN, M. 2011. HOT: Hodge-optimized triangulations. *ACM Trans. Graph. 30*, 4.

SCHAEFER, S., JU, T., AND WARREN, J. 2007. A unified, integral construction for coordinates over closed curves. *CAGD 24*, 8-9, 481–493.

SHEPARD, D. 1968. A two-dimensional interpolation function for irregularly-spaced data. In *ACM National Conference*, 517–524.

SIBSON, R. 1981. A brief description of natural neighbor interpolation. In *Interpolating Multivariate Data*. John Wiley & Sons, ch. 2, 21–36.

SUKUMAR, N., AND BOLANDER, J. 2009. Voronoi-based interpolants for fracture modelling. *Tessellations in the Sciences*.

SUKUMAR, N. 2004. Construction of polygonal interpolants: a maximum entropy approach. *Int. J. Num. Meth. Eng. 61*, 12, 2159–2181.

VARADY, T., SALVI, P., AND KARIKO, G. 2016. A multi-sided Bézier patch with a simple control structure. *Comp. Graph. Forum 35*, 2, 307–317.

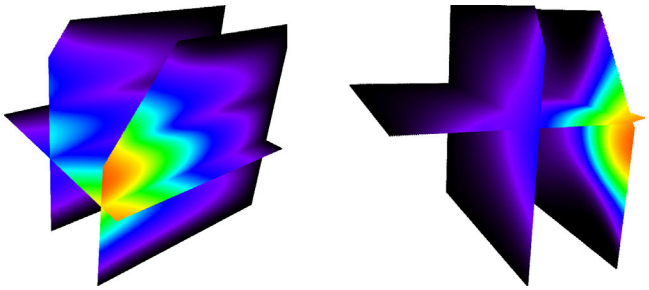

Figure 12: ***More 3D coordinates.*** *Left: anisotropic mean value coordinates for* $G = \mathrm{diag}(5\cos^2(10x)+1, 1, 1)$. *Right: iterated power coordinates from Eq.* (18) *in 3D.*

WACHSPRESS, E. 1975. *A Rational Finite Element Basis*. Academic Press.

WARREN, J., SCHAEFER, S., HIRANI, A. N., AND DESBRUN, M. 2006. Barycentric coordinates for convex sets. *Advances in Computational Mathematics 27*, 3, 319–338.

WARREN, J. 2003. On the uniqueness of barycentric coordinates. *Contemporary Mathematics*, 93–99.

WEBER, O., AND GOTSMAN, C. 2010. Controllable conformal maps for shape deformation and interpolation. *ACM Trans. Graph. 29*, 4, Art. 78.

WEBER, O., BEN-CHEN, M., AND GOTSMAN, C. 2009. Complex barycentric coordinates with applications to planar shape deformation. *Comp. Graph. Forum 28*, 2.

WEBER, O., BEN-CHEN, M., GOTSMAN, C., AND HORMANN, K. 2011. A complex view of barycentric mappings. *Comp. Graph. Forum 30*, 5, 1533–1542.

WEBER, O., PORANNE, R., AND GOTSMAN, C. 2012. Biharmonic coordinates. *Comp. Graph. Forum 31*, 8, 2409–2422.

ZHANG, J., DENG, B., LIU, Z., PATANÈ, G., BOUAZIZ, S., HORMANN, K., AND LIU, L. 2014. Local barycentric coordinates. *ACM Trans. Graph. 33*, 6, Art. 188.

A Lagrange & Facet Restriction Properties

We here show that conditions (a)-(d) imply properties (e) and (f) for the case of convex polytope $\mathcal{P}$ with vertices $\{\mathbf{v}_i\}_{i=1\ldots n}$ in arbitrary dimension. As a consequence of (a) and (b), we have $\sum_i \lambda_i(\mathbf{x})(\mathbf{v}_i - \mathbf{x}) = 0$. When evaluating at a vertex $\mathbf{v}_j$, one gets:

$$\sum_{i=1\ldots n, i\neq j} \lambda_i(\mathbf{v}_j)(\mathbf{v}_i - \mathbf{v}_j) = 0$$

Since all vertices are extreme points of the polytope, a convex combination of vectors $(\mathbf{v}_i - \mathbf{v}_j)_{i\neq j}$ is zero if and only if all the coefficients are zeros, i.e., $\lambda_i(\mathbf{v}_j) = 0$ for $i = 1\ldots n, i \neq j$: indeed, there exists a direction at $\mathbf{v}_j$ along which all vectors $(\mathbf{v}_i - \mathbf{v}_j)_{i\neq j}$ have positive components. Using condition (a), we conclude that the Lagrange property (e) holds, i.e., $\lambda_i(\mathbf{v}_j) = \delta_{ij}$.

As for condition (f), we can construct a coordinate system such that a given boundary facet contains vertices with their first coordinates at 0, and such that all other vertices have positive first coordinates due to the convexity of $\mathcal{P}$. Thus, similar to the previous argument, property (f) reflecting the restriction of coordinates to the boundary facets follows from conditions (a)-(d) since a positive linear combination of positive numbers must be a positive number.